CANCER BIOTHERAPY AND RADIOPHARMACEUTICALS
Volume 33, Number 8, 2018

DOI: 10.1089/cbr.2018.2494

Original Articles

Actinium-225 for Targeted α Therapy: Coordination Chemistry and Current Chelation Approaches

Nikki A. Thiele and Justin J. Wilson

Abstract

The α-emitting radionuclide actinium-225 possesses nuclear properties that are highly promising for use in targeted α therapy (TAT), a therapeutic strategy that employs α particle emissions to destroy tumors. A key factor, however, that may hinder the clinical use of actinium-225 is the poor understanding of its coordination chemistry, which creates challenges for the development of suitable chelation strategies for this ion. In this article, we provide an overview of the known chemistry of actinium and a summary of the chelating agents that have been explored for use in actinium-225-based TAT. This overview provides a starting point for researchers in the field of TAT to gain an understanding of this valuable therapeutic radionuclide.

Keywords: actinides, actinium-225, coordination chemistry, macrocyclic ligands, radiopharmaceuticals, targeted α therapy

Introduction

Targeted radionuclide therapy (TRT) is a powerful cancer treatment strategy that employs high-affinity tumor-targeting vehicles, such as antibodies, peptides, or small molecules, to deliver particle-emitting radionuclides to cancer cells, where they deposit a lethal payload of ionizing radiation (Fig. 1).[1,2] As a noninvasive, highly potent therapy in which off-target damage to noncancerous tissues is minimized, TRT is a valuable addition to the conventional treatment approaches of surgery, chemotherapy, and external beam radiation. The clinical utility of TRT has been validated by the FDA approvals of ^{90}Y-ibritumomab tiuxetan (Zevalin®) and ^{131}I-tositumomab (Bexxar®) in 2002 and 2003, respectively. These radioimmunotherapeutic agents consist of a CD20 antigen-targeting monoclonal antibody labeled with a β particle-emitting nuclide for the treatment of B-cell non-Hodgkin's lymphoma.[3]

Although β-emitting radiopharmaceutical agents have demonstrable efficacy for the ablation of tumors, their utility may be limited for some forms of metastatic cancer due to their physical characteristics.[4] Depending on their energy, β particles can travel up to a centimeter from the site of nuclear decay, which can result in the nonspecific irradiation of healthy tissues neighboring the targeted malignancy. β particles also possess low linear energy transfer (LET), or energy deposition per unit pathlength, which reduces their cytotoxic efficacy and necessitates the administration of high doses of radioactivity to achieve therapeutic benefits. Using β emitters, the targeting of individual cells, smaller tumor burdens, and micrometastases is impossible.

In addition to β particles, other forms of radioactive emissions may be leveraged for the destruction of tumor cells. In particular, α particles are promising alternatives to β particles (Fig. 1). In comparison to β particles, α particles travel much shorter distances in biological media and exhibit higher LET, making α-emitting radionuclides attractive for use in TRT.[4–6] The path length of an emitted α particle ranges from 40 to 100 μm, or a few cell diameters. Therefore, the radiotoxicity of α emitters is confined to the targeted site, giving rise to high specificity for tumor cells. Furthermore, α particles deposit a mean energy of 80 keV per μm traveled in biological tissue, a value that is several orders of magnitude larger than that for β particles. This high LET of α particles causes more ionization events per track, contributing to irreparable, lethal DNA double-strand breaks.[7] It is estimated that as little as one transversal of the cell nucleus by an α particle can sterilize a tumor cell,[8] signifying the high potency of these emissions. By contrast, hundreds to thousands of decay events are required to annihilate tumor cells using β particles.

Department of Chemistry and Chemical Biology, Cornell University, Ithaca, New York.

Address correspondence to: Justin J. Wilson; Department of Chemistry Baker Laboratory and Chemical Biology, Cornell University; Ithaca, NY 14850
E-mail: **jjw275@cornell.edu**

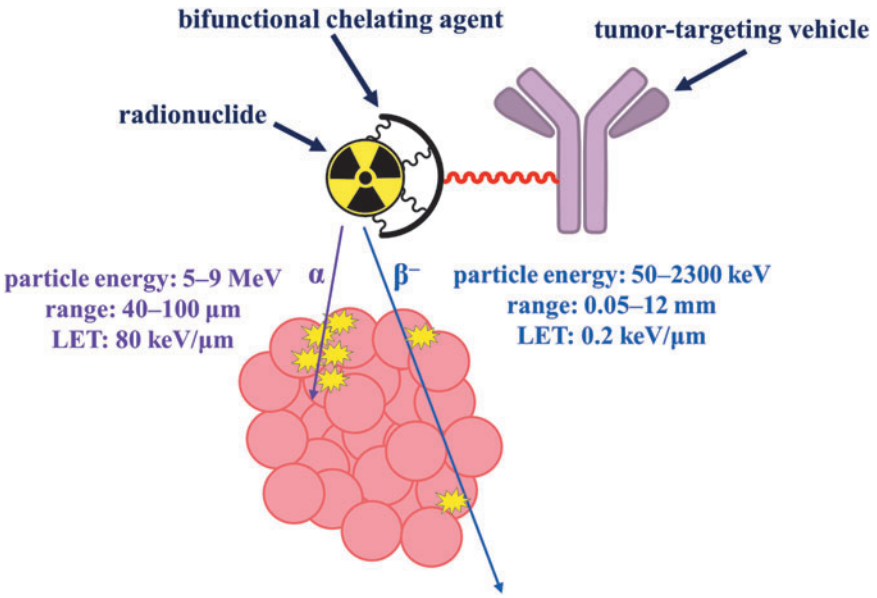

FIG. 1. Schematic diagram depicting the concept of targeted radionuclide therapy employing either alpha (α) or beta (β^-) particles in a tumor-targeting construct. The high LET and short range of α particles make them highly desirable for use in cancer therapy. LET, linear energy transfer.

Despite the unparalleled cytotoxicity of α particles, the development of α-emitting radiopharmaceuticals has been hampered by the limited supply and unresolved chemistry of α emitters, problems that are not present for conventional β-emitting nuclides. A major milestone for the use of α emitters in cancer therapy was achieved in 2013 when the first-in-class α-emitting therapeutic agent radium-223 dichloride ($^{223}RaCl_2$, Xofigo®) was brought to market.[9] As a bone-targeting calcium mimic, the $^{223}Ra^{2+}$ ion is administered in an unchelated form as the simple chloride salt for the treatment of bone metastases stemming from metastatic castration-resistant prostate cancer.[10,11] To be more generally utilized in targeted α therapy (TAT) applications[12–14] to treat a wide range of cancers in addition to bone metastases, however, α emitters must be conjugated to tumor-targeting scaffolds using bifunctional chelating agents,[15] following a similar design strategy as that employed in the β-emitting radiopharmaceuticals Zevalin and Bexxar.

Among the α particle-emitting ions that possess properties suitable for use in TAT, actinium-225 (^{225}Ac) is highly promising.[16–18] The radiological half-life of ^{225}Ac is 9.92 d,[19] which enables the distribution of this radionuclide to clinics far from the site of production. Furthermore, this long half-life is compatible for use with macromolecular targeting vectors, such as antibodies or nanoparticles, which exhibit extended circulation times *in vivo*. As it decays to stable ^{209}Bi, ^{225}Ac generates eight short-lived progeny, emitting a total of four high-energy α particles that deliver a lethal radiation dose to cancer cells (Fig. 2).[20] Notably, ^{225}Ac is significantly more potent than its daughter nuclide, ^{213}Bi, in both *in vitro* and *in vivo* models.[21–23] The superior efficacy of ^{225}Ac compared to ^{213}Bi is most likely due to its 313-fold longer half-life and 3 additional α particle emissions.

Despite the favorable nuclear properties and high cytotoxicity of ^{225}Ac for use in TAT, two key challenges have prevented ^{225}Ac from reaching its full clinical potential. First, the quantities of ^{225}Ac that can be produced via current strategies cannot support its large-scale clinical use. The primary source of ^{225}Ac is from the decay of ^{229}Th ($t_{1/2} = 7340$ years), which originates from reactor-bred ^{233}U that was generated in the United States during the 1960s.[24,25] This supply only amounts to ~1.7 Ci per year, which is not sufficient for a global medical application of this nuclide. Alternative production strategies employing high-energy accelerators at government-run labs are currently under investigation and will most likely provide a solution to this problem within the coming years.[26–30] The second challenge that has hindered the implementation of ^{225}Ac-TAT is the need for the stable retention of ^{225}Ac and its progeny to targeting vectors *in vivo*. The loss of ^{225}Ac or its daughters from the targeting vectors will give rise to nonspecific radiotoxic effects.

The challenge of stable retention stems both from a lack of suitable chelating agents for ^{225}Ac and from the α recoil

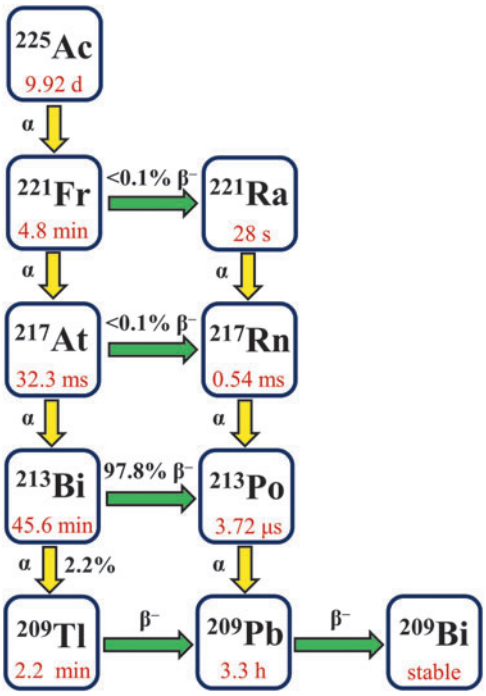

FIG. 2. Decay chain of ^{225}Ac.

effect, a phenomenon based on conservation of momentum laws that occurs upon release of an α particle. As described below, significant strides forward have been made in the development of chelators that form both thermodynamically stable and kinetically inert complexes with ^{225}Ac. The recoil effect, however, remains an insurmountable challenge with respect to conventional chelation strategies. The total amount of energy released upon α decay due to the daughter nuclide recoil exceeds that of 10,000 chemical bonds. As such, the daughter nuclides will always dissociate from the targeting construct upon their formation. Several approaches to contain ^{225}Ac and its daughters in nanoparticles have been explored with varying degrees of success.[31–38] The use of cell-internalizing targeting vectors may provide a strategy for retaining ^{225}Ac within cancer cells, where the daughter nuclides have limited mobility.[22]

Given the great interest in and value of ^{225}Ac as a therapeutic radionuclide in TAT, we present an overview of the chemistry of this element and the status of suitable chelating agents for the biological delivery of ^{225}Ac. Although there have been recent efforts to use nanoparticle-based delivery devices for this promising nuclide, our discussion will be limited to conventional bifunctional chelating agents.

Chemistry of Actinium

Background

Actinium, the lightest element in the actinide series, was first discovered by André Louis Debierne in 1899, and then several years later by Friedrich Oskar Giesel.[39] Since then, a total of 32 isotopes of actinium, ranging from ^{205}Ac to ^{236}Ac, have been identified or produced synthetically, and characterized. Of these isotopes, only ^{227}Ac and ^{228}Ac are present in nature as part of the naturally occurring decay chains of ^{235}U and ^{232}Th, respectively.[40,41] Within recent years, there has been a resurgence of interest in actinium, which has primarily been motivated by its potential use in TAT. This surge of interest, however, has outpaced the understanding of the chemistry of this element, which remains poorly developed owing to the limited supply and high radioactivity of all its isotopes. This incomplete understanding of the fundamental properties of actinium has slowed the development of novel chelation scaffolds, which are critical for the use of this nuclide in TAT. In this section, we summarize the known chemical and structural properties of the actinium ion, compiled in Table 1, and describe how these features can be leveraged for ligand design.

Aqueous chemistry

In aqueous solution, actinium exists most stably in the +3 oxidation state. There is some evidence, however, that the +2 oxidation state may also be accessible.[42] For example, in a radiopolarographic reduction study, a reduction half-wave potential was observed for aqueous solutions of $^{225}Ac^{3+}$. This potential shifted in the negative direction by $\sim$150 mV upon the addition of 18-crown-6. Based on these data, this half-wave potential was attributed to the formation of the +2 actinium ion.[43] Conversely, on the basis of poor extraction yields of ^{227}Ac with sodium amalgam in aqueous sodium acetate, an extraction procedure that is effective for lanthanides with stable +2 oxidation states, it was concluded that a +2 actinium ion is unlikely.[44] Additionally, theoretical studies predict highly negative standard reduction potentials of –4.9 V[45] and –3.3 V[46] relative to the normal hydrogen electrode for the Ac^{3+}/Ac^{2+} couple, suggesting that this reduction is impossible in aerobic aqueous media.

Table 1. Chemical and Structural Properties of Ac^{3+} and La^{3+}

Property[a]	*Ac^{3+}*	*La^{3+}*
6-Coordinate ionic radius (Å)	1.12	1.03
pK_{1h}	9.4	8.5
η (eV)	14.4	15.4
E_A	2.84	3.90
C_A	0.28	0.379
I_A	10.14	10.29
Hydration number	10.9 ± 0.5	9.2 ± 0.37
M–O_{H2O} (Å)	2.59(3)[b], 2.63(1)[c]	2.54(3)

[a]pK_{1h}, first hydrolysis constant; η, absolute chemical hardness; E_A, electrostatic contribution to the formation constants of Lewis acid-base complexes; C_A, covalent contribution to the formation constants of Lewis acid-base complexes; I_A, ionicity in bonding, E_A/C_A.
[b]Ref.[71].
[c]Ref.[72].

The Ac^{3+} ion possesses chemical properties that are similar to the lanthanide, Ln^{3+}, ions. Specifically, lanthanum, La^{3+}, is a suitable nonradioactive surrogate for the Ac^{3+} ion. Quantitatively, La^{3+} differs from Ac^{3+} by its smaller ionic radius. The six-coordinate ionic radius of La^{3+} is 1.03 Å, compared with 1.12 Å for Ac^{3+}.[47] Notably, Ac^{3+} is the largest +3 ion in the Periodic Table. As a result of its large size, it has correspondingly low charge density, a feature that makes Ac^{3+} the most basic +3 ion. Hydrolysis of the Ac^{3+} ion is observed between pH 8.6 and 10.4.[48–50] A precise value for the first hydrolysis constant (pK_{1h}) of Ac^{3+} was recently determined.[51] This constant expresses the ability of the Ac^{3+} ion to polarize a coordinated water molecule sufficiently to effect the release of a proton and formation of $AcOH^{2+}$. A pK_{1h} of 9.4 ± 0.1 was measured using an ion-exchange method. By contrast, the first hydrolysis constant of La^{3+} is 8.5.[49] The lower pK_{1h} of La^{3+} arises from the higher charge density of this ion, which more strongly favors the coordination of water and the subsequent release of a proton at a more acidic pH. An interesting aspect of the high pK_{1h} value for Ac^{3+} is that it indicates that hydrolysis does not occur until the pH is greater than 9. Thus, for radiolabeling considerations, basic buffers might prove to give effective radiochemical yields because little formation of the inert $AcOH^{2+}$ is expected.

Coordination chemistry

Metal-ligand bonding in actinium complexes is driven primarily by electrostatic interactions and steric constraints. Because the stability of electrostatic interactions scales as the ratio of charge over distance, the large ionic radius of the Ac^{3+} ion gives rise to the formation of kinetically labile complexes. Furthermore, the lack of significant ligand-field stabilization energy effects for this actinide ion afford a high degree of structural diversity in Ac-ligand complexes that is limited only by the coordinative saturation of the Ac^{3+} ion

and ligand–ligand steric interactions. Due to its lack of polarizability, Ac^{3+} is classified as a ''hard'' Lewis acid according to the Hard and Soft Acids and Bases (HSAB) theory,[52] and is therefore likewise predicted to prefer ''hard,'' nonpolarizable, electronegative Lewis bases such as anionic oxygen donors. The hard/soft acid-base properties of a specific ion can be quantified using the concept of absolute chemical hardness. The absolute chemical hardness (η) of an ion is given by $\eta = (I - A)/2$, where I is the ionization energy and A is the electron affinity of the species of interest.[53,54] Based on reported values for the third and fourth ionization energies of Ac,[55] the Ac^{3+} ion is characterized by an absolute chemical hardness of 14.4 eV. For comparison, the absolute chemical hardness of La^{3+} is 15.4 eV.[53,54] It should be noted that both values are intermediate on the whole spectrum of hard and soft ions. Appreciably soft ions, like Au^{+}, Ag^{+}, and Cu^{+}, exhibit absolute chemical hardness values that range from 5.7 to 6.3eV, whereas conventional hard ions, like Sc^{3+} and Al^{3+}, are characterized by absolute chemical hardness values of greater than 24eV.[53,54] Therefore, the hardness values for Ac^{3+} and La^{3+} confirm that these ions are most certainly not soft, but are not among the hardest ions in the Periodic Table either.

Another useful concept to think about regarding HSAB properties of an ion is its corresponding E and C values. These E and C values, originally developed by Drago,[56] are parameterized based on known bond dissociation enthalpies. The assumption in this model is that bond dissociation enthalpies arise from a combination of electrostatic interactions, as characterized by the constant E, and covalent interactions, as characterized by the constant C. This model was further expanded by Hancock and Marsicano[57,58] for predicting stability constants in aqueous solutions [Eq. (1)].

$$\log K_1 = E_A{}^{aq} \cdot E_B{}^{aq} + C_A{}^{aq} \cdot C_B{}^{aq} - D_A \cdot D_B \qquad (1)$$

In Equation (1), E_A and C_A are constants derived from experimental stability constant data that reflect the tendency of a cation or Lewis acid to engage in meaningful electrostatic or covalent interactions, respectively. E_B and C_B are the analogous parameters for a given ligand or Lewis base. The final terms, D_A and D_B, account for unfavorable steric interactions between the Lewis acid and base. Generally, for large ions, such as the third row transition metals, lanthanides, and actinides, this steric term is zero. In addition to having useful predictive power for stability constants, these E and C parameters can also be used to estimate the ionicity, I_A, of a given Lewis acid. This ionicity is taken as the ratio of the electrostatic and the covalent contributions to bonding, $I_A = E_A/C_A$. The ionicity can be interpreted as another quantitative measurement of chemical hardness, with a larger degree of ionicity corresponding to harder ions.

Based on known stability constants of Ac^{3+} with fluoride[42,59] and hydroxide,[48–51] the E and C values for this cation are calculated to be 2.84 and 0.28, respectively. The resulting ionicity is 10.14. The I_A value for Ac^{3+} is very close to that of La^{3+} ($I_A = 10.30$),[58] reinforcing the chemical similarity between these two ions. The individual values of E (3.90) and C (0.379) for La^{3+} are slightly greater than those of Ac^{3+}. The smaller ionic radius and larger charge density of La^{3+}, compared with Ac^{3+}, provides a rationale for the larger E value of this ion. The C values for these ions are similar, indicating that neither has a strong covalent component to their bonding interactions. Using Equation (1), the E and C values should be valuable for the prediction of Ac^{3+} stability constants with representative ligands, which may aid in ongoing ligand design strategies.

Experimental conditional stability constants have been measured for several simple complexes of Ac^{3+}.[42,59–64] These measurements are typically carried out using liquid–liquid extraction techniques at a fixed acidic pH using extractants, such as di-(2-ethylhexyl)phosphoric acid or dinonylnaphthylsulfonic acid, in the organic phase. From these studies, several trends are apparent. First, Ac^{3+} forms monohalido complexes of decreasing stability as heavier halides are employed. The stability constant β_1, where $\beta_n = [ML_n]/[M][L]^n$, is $\sim$500–1000 times larger for the formation of AcF^{2+} compared to the formation of either $AcCl^{2+}$ or $AcBr^{2+}$. This large thermodynamic preference for F^- is consistent with the HSAB properties of this ion, as discussed above. The absolute chemical hardness of F^- ($\eta = 7.0$) is significantly greater than that of Cl^- ($\eta = 4.7$) or Br^- ($\eta = 4.2$).[53] As such, the fluoride ion is predicted to coordinate more strongly to hard acids like Ac^{3+}. The Ac–F complex ($\beta_1 \approx 529$) is also more stable than Ac^{3+} complexes of NO_3^- ($\beta_1 = 1.31$), SO_4^{2-} ($\beta_1 = 15.9$–22.9), and $H_2PO_4^-$ ($\beta_1 = 38.8$). For these latter three inorganic anions, the stability constants increase with the basicity of the anion. Multidentate organic ligands predictably give rise to more stable Ac^{3+} complexes. For example, the stability constant for the formation of the citrate complex of Ac^{3+} is 9.55×10^6.[42] The complex of Ac^{3+} and EDTA is even more stable ($\beta_1 = 1.66 \times 10^{14}$).[65] The greater complex stability can be attributed to the higher denticity of EDTA, a hexadentate ligand, compared with citrate, a tridentate ligand. Ac^{3+} stability constants are similar to those of La^{3+}, but usually slightly lower.[60–63,66,67] The smaller Ac^{3+} stability constants are a consequence of the large radius of this ion, which gives rise to weaker electrostatic interactions with the ligand donor atoms.

Structural chemistry

An understanding of the structural chemistry of Ac^{3+} also provides useful information about the coordination preferences of this ion, insight that is of value in the design of new chelation platforms. The structural characterization of the Ac^{3+} ion, however, has been hindered by the lack of long-lived isotopes. The longest-lived isotope, ^{227}Ac, has a half-life of only 22 years. The short half-life, limited availability, and radiological hazards of this isotope have challenged characterization techniques, such as X-ray crystallography, which require macroscopic quantities. Furthermore, the absence of appreciable spectroscopic features of this $5f^0$ $6d^0$ ion limits the use of optical spectroscopy techniques.

A series of actinium complexes have been characterized by X-ray powder diffraction, a technique that can be applied on microcrystalline powder samples. The solid-state compounds AcF_3, $AcCl_3$, $AcBr_3$, AcOF, AcOCl, AcOBr, Ac_2O_3, Ac_2S_3, and $AcPO_4 \cdot 0.5H_2O$ were all characterized in a single study published nearly 70 years ago.[68] Likewise, $Ac_2(C_2O_4)_3 \cdot 10H_2O$ and AcH_3 were prepared and characterized based on their powder patterns.[69,70] For all of these compounds, the powder pattern was comparable to that obtained for the La^{3+} analogs, indicating that the Ac^{3+} structures are

isomorphous to those of La^{3+}. This result is consistent with the chemical similarity of these ions, as described above. Furthermore, although direct Ac–L bond distances could not be measured, the unit cells determined from the Ac^{3+} diffraction patterns were consistently larger than those of La^{3+}, reflecting the larger ionic radius of Ac^{3+}. The data afforded by X-ray powder diffraction, however, is not significantly meaningful with respect to determining precise coordination geometries about Ac^{3+} centers.

In 2016, the first Ac–L bond distances were measured by extended X-ray absorption fine-structure (EXAFS) spectroscopy.[71] These experiments employed ^{227}Ac in aqueous solutions, taking advantage of the high sensitivity of the fluorescence detection mode of this spectroscopic technique. A solution of Ac^{3+} in aqueous HCl revealed photoelectron backscattering components that were assigned to inner-sphere Ac–O_{H2O} and Ac–Cl interactions. The interatomic distances were measured to be 2.59(3) and 2.95(3) Å for the Ac–O_{H2O} and Ac–Cl bonds, respectively. A subsequent follow-up study characterized the homoleptic Ac-aquo complex.[72] The results from this EXAFS study reveal 10.9 ± 0.5 inner-sphere water molecules coordinated to the Ac^{3+} center. The average Ac–O_{H2O} bond length was measured to be 2.63(1) Å. By comparison, the La-aquo complex bears 9.2 ± 0.37 inner-sphere water molecules, with an average La–O_{H2O} bond length of 2.54(3) Å.[73] The higher hydration number and longer metal-oxygen bond length found in the Ac-aquo complex versus the La-aquo complex is a consequence of the larger size of the Ac^{3+} ion, which can accommodate more ligands in its inner coordination sphere. Furthermore, among homoleptic aquo complexes, the Ac-aquo complex is the only example of an 11-coordinate structure. These results highlight how Ac^{3+}, as the largest +3 ion, may exhibit unexpected and divergent chemistry from the lanthanides and provide a promising first glimpse into the coordination chemistry of actinium. Ongoing EXAFS studies to characterize coordination complexes of Ac may reveal critical structural features that dictate complex stability.

Bifunctional Ligands for the Chelation of Actinium

Background

For the successful implementation of TAT with ^{225}Ac, this radionuclide must be delivered with high specificity and retained within the vicinity of targeted cancer cells over the course of its nuclear decay. These conditions are best accomplished by covalently linking a tumor-targeting vector to a bifunctional chelator that forms a thermodynamically and kinetically stable complex with the $^{225}Ac^{3+}$ ion. Unfortunately, the development of effective bifunctional chelating agents for $^{225}Ac^{3+}$ has been hindered by the poorly understood coordination chemistry of this short-lived radioactive ion. This lack of knowledge regarding Ac^{3+} coordination chemistry makes it difficult to accurately foresee which ligands will form stable complexes *in vitro* and *in vivo*. Another challenge in the design of ligands for Ac^{3+} is the large ionic radius of this ion, which gives rise to a low charge-to-ionic radius ratio, a feature that leads to weaker electrostatic interactions with ligands.

In vivo, the instability of ^{225}Ac-ligand complexes is reflected by the accumulation of free ^{225}Ac in the liver and bone, where its radioactive emissions give rise to acute radiotoxic effects.[74,75] As such, the formation of kinetically inert complexes of ^{225}Ac is a crucial prerequisite for the application of this radionuclide for TAT. In this section, we will describe research efforts to develop an effective bifunctional chelating agent for ^{225}Ac. Specifically, the application of DOTA (Fig. 3) as the current state of the art for the chelation of the Ac^{3+} ion and the use of alternative chelating agents for this radionuclide are discussed.

DOTA: the current gold standard

DOTA is a 12-membered macrocycle that provides octadentate coordination via 4 tertiary amine nitrogen donors and 4 carboxylic acid pendent arms (Fig. 3). This ligand is widely employed for the stable chelation of other tripositive radiometals such as $^{68}Ga^{3+}$, $^{111}In^{3+}$, $^{177}Lu^{3+}$, $^{86/90}Y^{3+}$, and $^{44/47}Sc^{3+}$,[15] and is a critical component of FDA-approved peptide constructs for the diagnosis (^{68}Ga-DOTATATE) and treatment (^{177}Lu-DOTATATE) of somatostatin receptor-positive neuroendocrine tumors. With its established clinical efficacy that demonstrates its ability to stably coordinate chemically hard +3 ions, DOTA is expected to provide a suitable chelating scaffold for the Ac^{3+} ion.

In an initial study that examined the biodistribution of ^{225}Ac-DOTA in normal BALB/c mice, the complex rapidly cleared from the blood; only a slight accumulation of activity was observed in the liver and bone of mice after 5 d (3.29%ID/g and 2.87%ID/g, respectively).[76] These results suggest that the ^{225}Ac-DOTA complex is sufficiently stable *in vivo*, prompting further studies on the ^{225}Ac-chelation efficacy of DOTA in tumor-targeting antibody constructs.[22] Initial efforts to prepare ^{225}Ac-DOTA-antibody constructs

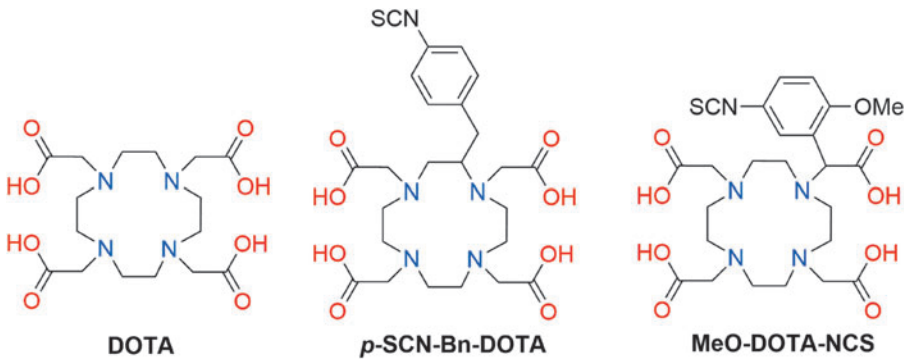

FIG. 3. Structures of DOTA and its bifunctional derivatives.

required a two-step procedure.[77] First, both *p*-SCN-Bn-DOTA and MeO-DOTA-NCS (Fig. 3) were radiolabeled with ^{225}Ac at 55–60°C for 30 min in pH 5 acetate buffer. Under these conditions, no differences in radiolabeling efficiencies were observed between the two bifunctional DOTA ligands; both yielded the expected ^{225}Ac-DOTA-NCS complexes, which were used interchangeably for the following bioconjugation step.

In the second step, ^{225}Ac-DOTA-NCS was conjugated to a monoclonal antibody using the isothiocyanate (NCS) functional group, which reacts with lysine residues on the antibody to form stable thiourea linkages. This two-step procedure was necessary because temperature-sensitive antibodies cannot tolerate the 55°C–60°C temperature required to incorporate Ac^{3+} into the DOTA macrocycle. This process was successfully employed for the preparation of ^{225}Ac-DOTA constructs with the antibodies HuM195 (anti-CD33), B4 (anti-CD19), trastuzumab (anti-HER2/neu), and J591 (anti-PSMA, prostate-specific membrane antigen), which target leukemia, lymphoma, breast/ovarian cancer, and prostate cancer, respectively.[22] Greater than 95% of the ^{225}Ac-DOTA-J591 construct remained intact after incubating in human serum for 15 d. Furthermore, all of the conjugates retained their biological activities, as they were readily internalized by cancer cells and gave rise to potent cytotoxic effects. The *in vivo* efficacies of ^{225}Ac-DOTA-J591 and ^{225}Ac-DOTA-B4 were evaluated in mice bearing either solid prostate carcinoma or disseminated human lymphoma, respectively. In both models, single doses of the ^{225}Ac-labeled constructs led to tumor regression and prolonged survival of mice compared with untreated controls. From this pivotal study, ^{225}Ac was established as a feasible radionuclide to deliver a series of lethal α particles to cancer cells, leading to its designation as an ''atomic nanogenerator.''

The utility of DOTA as a bifunctional chelating agent for ^{225}Ac-TAT constructs has subsequently been investigated in numerous preclinical studies that have shown promising results for the treatment of a range of different cancers.[78–86] Notably, ^{225}Ac-DOTA constructs are currently being evaluated in several clinical trials for the treatment of leukemia, multiple myeloma, and prostate cancer.[87–90] These trials, which have demonstrated the incredible therapeutic potential of this radionuclide in humans (Fig. 4), have garnered great interest for ^{225}Ac-TAT.

Despite these advances in the field of ^{225}Ac-TAT, the ^{225}Ac-chelation properties of DOTA are not optimal for use in this application. Thermodynamically, the stability of metal ion complexes of DOTA is inversely related to the ionic radius of the metal ion, with larger metal centers giving rise to less stable complexes.[91,92] The thermodynamic preference of DOTA for smaller ions puts Ac^{3+} at a notable disadvantage, given its status as the largest +3 ion. In addition to thermodynamic considerations, the kinetic inertness of radiometal-ligand complexes is another important factor that dictates the suitability of chelating agents for TAT. Radiopharmaceuticals are administered in very low doses and are thus subject to highly dilute conditions *in vivo*, circumstances that enhance the off-rate kinetics of a radiometal-ligand complex. In this context, several studies have called into question the kinetic stability of ^{225}Ac-DOTA constructs, as they report the loss of ^{225}Ac from DOTA both *in vitro*[77] and *in vivo*.[76]

In addition to the off-rate kinetics, the on-rate kinetics, which dictate the rate at which radiolabeling occurs, also present a major challenge to the widespread use of DOTA in the clinic for ^{225}Ac-TAT. Complete radiolabeling of DOTA conjugates with $^{225}Ac^{3+}$ in short periods of time requires the application of high temperatures.[22,77,78,81,83,93] As such, the two-step labeling procedure,[77] as described above, has been applied for labeling antibodies with ^{225}Ac to avoid directly subjecting them to temperatures above 37°C that lead to their denaturation.

Recently, a one-step method has been developed for the formation of ^{225}Ac-DOTA-antibody constructs in which DOTA-antibody conjugates are directly radiolabeled with ^{225}Ac at 37°C for 2 h.[84] This procedure offers several key advantages over the two-step method. For example, 10-fold higher radiochemical yields and 30-fold higher specific activities are observed for the one-step compared to the two-step radiolabeling methodology. Ideally, however, rapid radiolabeling (<20 min) at room temperature would greatly facilitate the use of ^{225}Ac in the clinical setting and minimize radiolytic damage to sensitive antibody-based targeting vectors, ultimately improving specific activity while maintaining immunoreactivity. Aside from the 2 h one-step labeling of

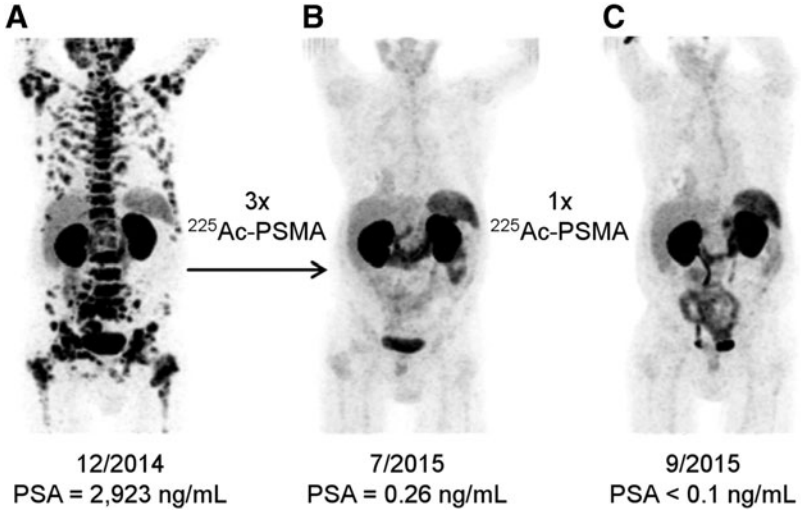

FIG. 4. ^{68}Ga-PSMA-11 PET/CT scans of a patient with metastatic castration-resistant prostate cancer before **(A)** and after **(B, C)** receiving several cycles of ^{225}Ac-PSMA-617, a small-molecule construct. Complete imaging response and a remarkable reduction in prostate-specific antigen, a biomarker for prostate cancer, were achieved after the final treatment, demonstrating the extraordinary potential of ^{225}Ac for TAT. This figure was reprinted with permission from ref. 89. Copyright © 2016 by the Society of Nuclear Medicine and Molecular Imaging, Inc. TAT, targeted α therapy.

DOTA with ^{225}Ac just described, no other more rapid or mild radiolabeling conditions have been discovered for this ligand. Collectively, these shortcomings indicate that DOTA is not ideal for use in ^{225}Ac-TAT applications, highlighting the need for more suitable chelating scaffolds for ^{225}Ac.

Aminocarboxylate and aminophosphonate ligands

Because of the limitations of DOTA, alternative ligands have been explored for the chelation of the $^{225}Ac^{3+}$ ion for TAT. Early efforts to discover effective ^{225}Ac-chelating agents were directed toward the evaluation of linear polyaminocarboxylate and polyaminophosphonate ligands, and other low molecular weight compounds, such as citrate.[75,94–96] Acyclic ligands are appealing for use in radiopharmaceuticals because they generally exhibit rapid radiolabeling kinetics, which permits incorporation of radiometals at room temperature within minutes.[15] The investigation of this class of ligands with ^{225}Ac, however, revealed that they did not form kinetically inert complexes. For example, the biodistribution of ^{225}Ac complexes of EDTA, a hexadentate ligand, and CHX-A″-DTPA, an octadenate ligand (Fig. 5), in mice revealed significant accumulation of radioactivity in the liver and bone, consistent with the biodistribution pattern of unchelated Ac^{3+}.[75,76] Notably, the Ac^{3+} complex of EDTA is ~75% less stable than that of CHX-A″-DTPA,[75] a property that may be attributed to the fewer number of ligand donor atoms available for EDTA to coordinate the Ac^{3+} ion. Moreover, the preorganized diamino cyclohexyl group in the backbone of CHX-A″-DTPA may further increase the stability of the ^{225}Ac complex, compared to the nonrigid ethylenediamine backbone of EDTA.

Additional preorganization in the form of macrocycles (the macrocyclic effect) significantly improves the stability of ^{225}Ac-ligand complexes in mice.[76] For example, the ligand HEHA (Fig. 5), which is structurally related to DOTA by virtue of their polyaza macrocyclic cores that bear pendent carboxylate arms, was also found to be effective for Ac^{3+} chelation. HEHA differs from DOTA in the size of its macrocyclic cavity and in the number of nitrogen and oxygen donor atoms that it possesses; DOTA (N_4O_4) is a 12-membered macrocycle and HEHA (N_6O_6) is an 18-membered macrocycle. As noted above, for the DOTA complex, a slight accumulation of ^{225}Ac was observed in the liver and bone of mice after 5 d (3.29%ID/g and 2.87%ID/g, respectively). This liver and bone accumulation, however, was dramatically less than that seen for the acyclic chelators EDTA (85.94%ID/g and 10.3%ID/g, respectively) and CHX-A″-DTPA (23.9%ID/g and 4.18%ID/g, respectively) over the same period of time.[75,76]

Notably, the HEHA complex of Ac^{3+} is slightly more stable *in vivo* compared to that of DOTA; only a negligible quantity (<0.3%ID/g) of radioactivity was detected in any organ after 5 d.[76] These results suggest that the larger 18-membered macrocyclic cavity of HEHA may be better matched to the large size of the Ac^{3+} ion than the 12-membered macrocyclic cavity of DOTA, giving rise to a more stable complex with $^{225}Ac^{3+}$. Another contributing factor to the slightly higher *in vivo* stability of ^{225}Ac-HEHA may be the greater denticity of this ligand compared to DOTA. The EXAFS studies of the Ac-aquo complex, described above, indicate that the Ac^{3+} ion can accommodate very high coordination numbers.[72] Hence, the 12 donor atoms of HEHA may more effectively saturate the coordination sphere of the Ac^{3+} ion compared to the 8 donor atoms of DOTA.

The bifunctional analog of HEHA, HEHA-NCS (Fig. 5), was subsequently prepared and conjugated to several different monoclonal antibodies. These HEHA-antibody conjugates were radiolabeled with ^{225}Ac and evaluated for stability.[97] When tested in fetal bovine serum, all of the ^{225}Ac-HEHA conjugates were unstable, as reflected by their >50% decomposition after 24 h. This instability was attributed to a combination of radiolytic decomposition of the ^{225}Ac-HEHA conjugates and transchelation of $^{225}Ac^{3+}$ by serum proteins. An ^{225}Ac-HEHA conjugate of

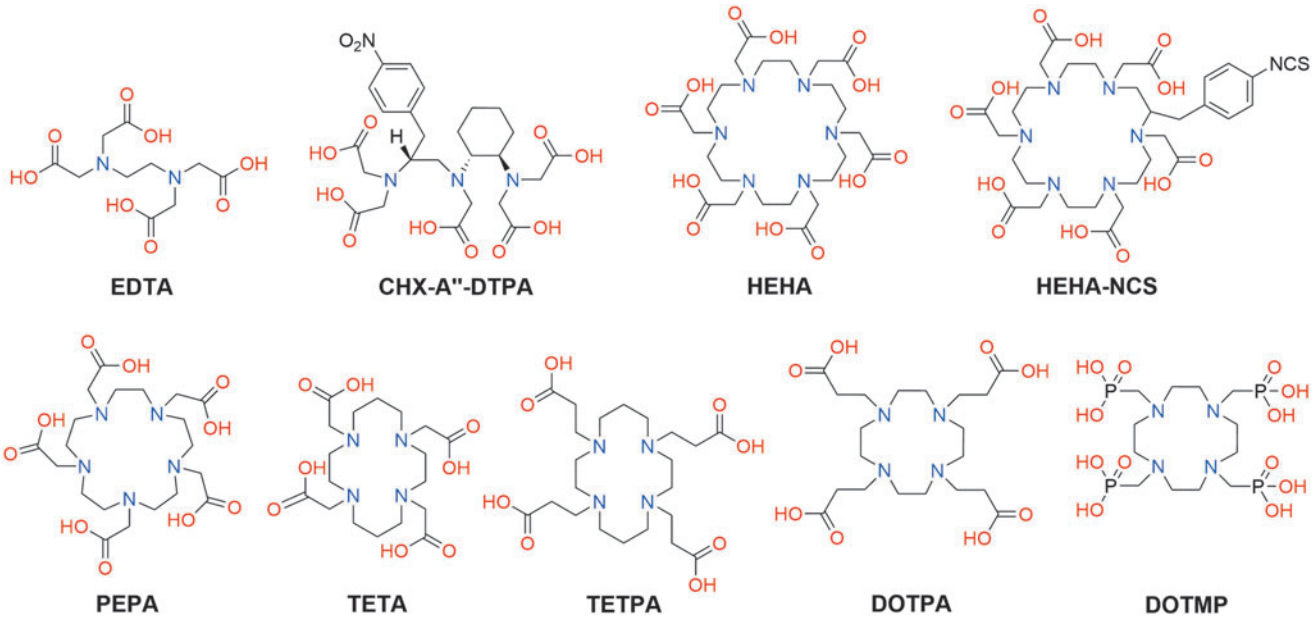

FIG. 5. Structures of acyclic and macrocyclic aminocarboxylate and aminophosphonate ligands investigated for the chelation of ^{225}Ac.

the thrombomodulin-binding monoclonal antibody 201B, which targets lung vasculature, was subsequently prepared and evaluated.[98] In normal mice treated with this construct, significant accumulation of ^{225}Ac was observed in the liver and bone after 6 d, signifying the loss of this radionuclide from the HEHA conjugate. For mice bearing lung tumor colonies, the construct was effective in destroying the cancer cells, but also gave rise to severe radiotoxicity. This toxicity was attributed to the loss of ^{225}Ac from HEHA due to both the instability of the chelate and the release of daughter nuclides arising from the α recoil effect. Although these results highlight the lack of long-term *in vivo* stability of Ac-HEHA complexes, it should be noted that the thrombomodulin-binding antibody does not enter cells.

Therefore, the use of cell-internalizing targeting vectors may minimize the redistribution of ^{225}Ac and its daughters, avoiding the associated downstream toxic side-effects. Furthermore, the significant difference in stability between the unfunctionalized ^{225}Ac-HEHA complex and the antibody-conjugated ^{225}Ac-HEHA complex underscores the importance of evaluating long-term stability of chelating agents with targeting vectors that will prolong *in vivo* circulation time.

In addition to DOTA and HEHA, several other macrocycles have been investigated for their Ac-chelation properties (Fig. 5). PEPA is a 15-membered polyaza macrocycle that provides decadentate coordination via 5 tertiary amine nitrogen donors and 5 carboxylic acid pendent arms. Despite possessing a macrocyclic core that is intermediate in size between DOTA and HEHA, PEPA was not able to form complexes that stably retained ^{225}Ac *in vivo*.[75] The striking difference between the stability of ^{225}Ac complexes of DOTA and HEHA versus PEPA is not readily explained based on a comparison of the ligand structures, emphasizing the critical need to develop a better understanding of the coordination chemistry of actinium.

The macrocycles TETA, TETPA, and DOTPA (Fig. 5) did not strongly bind ^{225}Ac in initial radiolabeling experiments and were therefore not investigated further.[77] TETA and TETPA are based on a cyclam macrocyclic core, which forms two 6-membered chelate rings upon metal coordination. The DOTPA ligand, which is based on a cyclen macrocycle like DOTA, bears four pendent carboxylate donors that are each linked to the macrocycle via a two-carbon chain. As such, these pendent donors form six-membered chelate rings upon metal coordination. By contrast, DOTA and HEHA, ligands that form complexes of higher stability with $^{225}Ac^{3+}$, only generate five-membered chelate rings upon metal ion coordination. As previously documented, large ions form thermodynamically more stable complexes with ligands that give rise to smaller chelate rings.[99] Thus, for Ac^{3+}, the largest +3 ion in the Periodic Table, there is a strong aversion to the larger six-membered chelate rings afforded by TETA, TETPA, and DOTPA. DOTMP (Fig. 5), an analog of DOTA in which the carboxylic acid pendent arms are replaced by phosphonic acid pendent arms, binds more strongly to ^{225}Ac than does TETA, TETPA, and DOTPA, but rapidly releases this radionuclide in human serum.[77] The drop in kinetic stability in moving from DOTA to DOTMP can be ascribed to the lower basicity of the phosphonate donors in the latter, a property that can often be correlated to ligand-metal donor strength.

Calixarenes and texaphyrins

Another class of macrocycles, calixarenes, have also been investigated as chelators for ^{225}Ac. A *tert*-butylcalix[4]arene possessing four acetic acid arms appended to the phenolic groups of the core scaffold (Fig. 6) complexes ^{225}Ac effectively, as demonstrated by its ability to nearly quantitatively extract this radionuclide from the aqueous phase in liquid–liquid extractions.[100] Additionally, the resulting ^{225}Ac-calix[4]arene complex remained intact over the course of 5 h in the presence of high concentrations of competing alkali and alkaline earth metal ions. Based on these promising studies, a derivative of this calix[4]arene tetracarboxylic acid bearing an amine-reactive isothiocyanate was prepared.[101] The further exploration of the utility of this ligand as a bifunctional chelator for ^{225}Ac, however, was not investigated. The synthesis of two other bifunctional calix[4]arene tetracarboxylic acid-based ligands have also been reported.[102] One of these ligands was successfully conjugated to human serum albumin and to the monoclonal antibody 506-A, which targets the pregnancy hormone hCG, but was ultimately not evaluated with ^{225}Ac.[102] Overall, these studies suggest that calix[4]arene-based scaffolds may be useful for ^{225}Ac chelation, but further investigations are needed to fully explore the potential of these ligands.

Aromatic or pi-conjugated macrocycles may also possess suitable properties for chelating radiometals. Specifically, the class of expanded porphyrins, known as texaphyrins, bind strongly to large f-element ions and exhibit tumor-selective uptake properties.[103] With respect to Ac^{3+} chelation, motexafin (Fig. 6), a therapeutically relevant texaphyrin, was predicted by density functional theory calculations to form highly stable complexes with this large ion.[104] Experimental studies, however, were not able to confirm this prediction. Under high-temperature radiolabeling conditions (90°C), no ^{225}Ac was incorporated into the texaphyrin, indicating that the N_5 donor system of this ligand is not effective for the

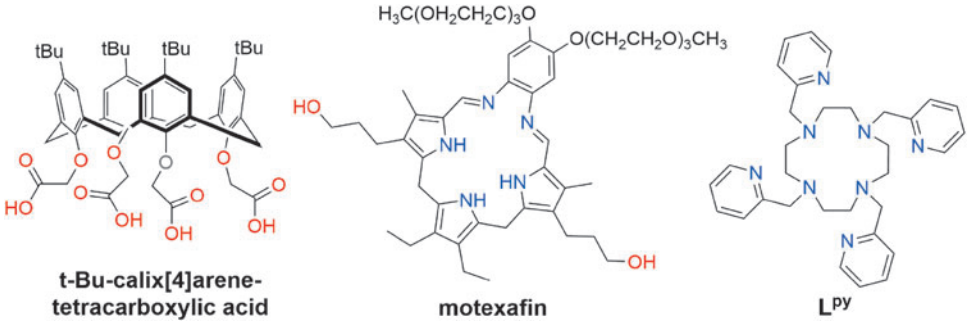

FIG. 6. Structures of *t*-Bu-calix[4]arene-tetracarboxylic acid, motexafin, and L^{py}.

chelation of the Ac^{3+} ion.[105] By contrast, its daughter nuclide ^{213}Bi was rapidly complexed by this macrocycle, consistent with results demonstrating the formation of cold Bi-texaphyrin complexes.[106]

The preferential binding of motexafin to the ^{213}Bi daughter nuclide of ^{225}Ac is a phenomenon that was previously observed for another nitrogen-rich macrocyle, L^{py} (Fig. 6).[107] This ligand carries the same 12-membered cyclen core as DOTA but bears pendent nitrogen-donor picolyl ligands, thereby providing an N_8 coordination sphere. Because L^{py} is structurally analogous to DOTA in that it only forms five-membered chelate rings, the large preference of this ligand for Bi^{3+} over Ac^{3+} was postulated to arise as a consequence of the nitrogen-rich coordination sphere provided by this ligand. Namely, the Ac^{3+} ion has a poor affinity for nitrogen donor atoms compared with the Bi^{3+} ion, which has a high affinity for these ligands. As such, these results highlight the need for the presence of chemically hard oxygen donor atoms in the development of $^{225}Ac^{3+}$ chelators.

Recent advances in the development of ^{225}Ac chelators

More recent studies have disclosed promising new candidates for ^{225}Ac chelation. Bispa^2 is an octadentate ligand bearing two picolinic acid pendent arms attached to the tertiary amine nitrogen atoms of a bispidine scaffold (Fig. 7).[108] In radiolabeling experiments, bispa^2 (10^{-4} M) completely complexed ^{225}Ac (40 kBq) at room temperature in under 30 min. Radiochemical yields decreased to 94%, 64%, and 2%, respectively, when lower ligand concentrations of 10^{-5}, 10^{-6}, and 10^{-8} M were used. Challenge experiments to assess the stability of the resulting ^{225}Ac complex of bispa^2 were carried out in human serum or in an aqueous solution containing fivefold excess of La^{3+}, with respect to ligand concentration, as a competing ion. Under these conditions, ~90% and 72% of ^{225}Ac-bispa^2 remained intact over the course of 7 d in human serum or in the presence of La^{3+}, respectively. These preliminary studies point toward the potential utility of bispa^2 for ^{225}Ac chelation; further *in vivo* studies employing biological targeting vectors are required, however, to establish the suitability of this ligand for ^{225}Ac-TAT.

Ligands based on the diaza-18-crown-6 macrocycle have also been subjected to investigations for ^{225}Ac chelation. For example, the ligand macropa (Fig. 7), which bears two pendent picolinate arms on the amine nitrogen atoms of the macrocyclic core, was probed for its ability to complex this large radiometal.[109] A unique feature of macropa, which prompted the studies with ^{225}Ac, is that it forms more stable complexes with large over small lanthanide ions.[110] Because Ac^{3+} has similar chemical properties as the lanthanides but is otherwise substantially larger, it was hypothesized that macropa would be a highly effective chelating agent for this ion. Radiolabeling of macropa with ^{225}Ac (26 kBq) gave quantitative radiochemical yields after 5 min at room temperature with ligand concentrations as low as 0.59 μM. Furthermore, the stability of the ^{225}Ac-macropa complex in an aqueous solution containing 50-fold excess of competing La^{3+} ions, with respect to ligand concentration, or in human serum was excellent; in both of these challenges, the ^{225}Ac-macropa complex remained intact for over 7 d. Upon injection of the ^{225}Ac-macropa complex into mice, no accumulation of activity in the liver or bone, signs of complex instability, was observed over the course of 5 h.

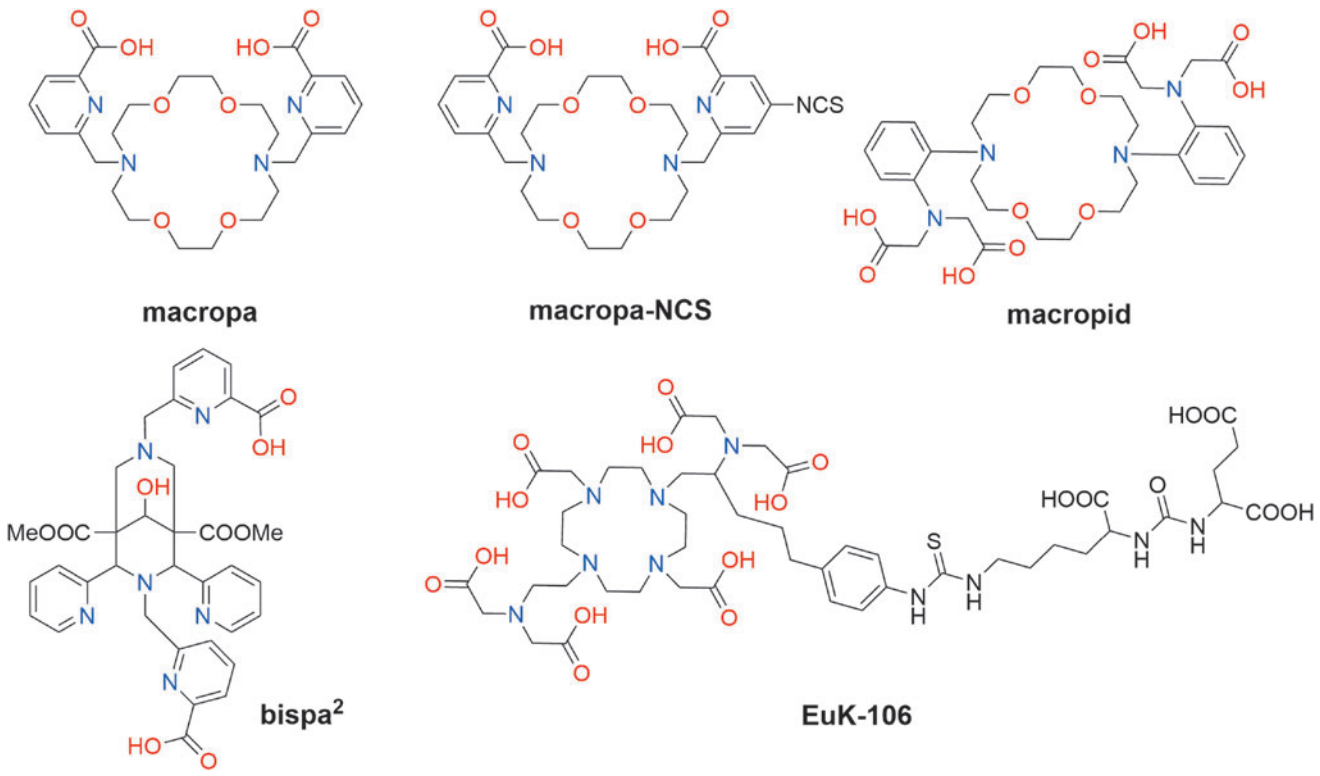

FIG. 7. Ligands investigated recently for the chelation of ^{225}Ac.

Based on these promising results, a bifunctional analog of macropa, macropa-NCS (Fig. 7), was synthesized, and it was conjugated to the antibody trastuzumab and to a small-molecule PSMA-targeting agent. The macropa-trastuzumab conjugate complexed ^{225}Ac in quantitative radiochemical yield at room temperature, marking a distinct advantage over antibody conjugates of DOTA, which are unable to complex ^{225}Ac under these conditions. The PSMA-targeting conjugate of macropa was similarly labeled with ^{225}Ac under mild conditions. The ^{225}Ac-labeled PSMA-targeting construct was administered to mice bearing prostate cancer xenografts. After 4 d, accumulation of ^{225}Ac was only observed in the tumor, indicating that macropa can stably retain this nuclide *in vivo* over an extended period of time. Based on these results, macropa is a highly promising chelating agent for ^{225}Ac that has key advantages over DOTA, which will favor its use for TAT.

Macropid (Fig. 7), another ligand based on the diaza-18-crown-6 macrocycle, was also evaluated for ^{225}Ac chelation (Thiele NA, Brown V, Kelly JM, et al., Unpublished Results, 2017). This ligand, which bears two phenyliminodiacetate pendent arms, was shown to exhibit selectivity for large over small alkaline earth metal ions.[111] Macropid provides a total of 12 donor atoms, exceeding the 10 donor atoms provided by macropa. Attempts to radiolabel this ligand with ^{225}Ac, however, were unsuccessful, even when high temperature conditions were applied. Likewise, EuK-106^{93} (Fig. 7), a PSMA-targeting conjugate comprising a DOTA-like scaffold bearing additional carboxylic acid donor atoms,[112] failed to complex ^{225}Ac under the high temperature conditions employed. Collectively, these results suggest that simply increasing the number of donor atoms in a ligand does not always increase the affinity for a large ion like Ac^{3+}.

Conclusions

The use of ^{225}Ac for TAT is an incredibly promising strategy for the development of new therapeutic radiopharmaceutical agents. Discussed above, a key challenge in the implementation of this nuclide in the clinic arises from its poorly understood coordination chemistry, which hinders the development of appropriate bifunctional chelating agents. In this review, we have highlighted the known coordination chemistry properties of this radioactive ion and summarized the chelation approaches that have been explored. A key feature of the Ac^{3+} ion that needs to be emphasized is its large ionic radius. The most successful ligands to date (DOTA, macropa) possess chelating scaffolds that can sufficiently accommodate the large size of this ion. The future development of ^{225}Ac-based radiopharmaceutical agents will require the further exploration of these classes of ligands. Lastly, the rigorous EXAFS studies of this elusive ion that are ongoing will most certainly provide a greater insight into its coordination chemistry, bridging an important gap between our knowledge of the actinides and their practical utility.

Acknowledgments

The authors acknowledge funding support from a Pilot Award from the Weill Cornell Medical College Clinical and Translational Science Center, funded by NIH/NCATS UL1TR00457.

Disclosure Statement

N.A.T. and J.J.W. are inventors on a patent application 62/478,945, submitted by Cornell University, which covers a method for the use of the ligand macropa for actinium-225-based alpha therapy. This technology has been licensed to Noria Therapeutics, where J.J.W. is a member of the scientific advisory board.

References

1. Dash A, Knapp FF, Pillai MRA. Targeted radionuclide therapy—An overview. Curr Radiopharm 2013;6:152.
2. Gudkov SV, Shilyagina NY, Vodeneev VA, et al. Targeted radionuclide therapy of human tumors. Int J Mol Sci 2016;17:33.
3. Milenic DE, Brechbiel MW. Targeting of radio-isotopes for cancer therapy. Cancer Biol Ther 2004;3:361.
4. Kassis AI, Adelstein SJ. Radiobiologic principles in radionuclide therapy. J Nucl Med 2005;46:4S.
5. Sgouros G. Alpha-particles for targeted therapy. Adv Drug Deliv Rev 2008;60:1402.
6. Sgouros G, Roeske JC, McDevitt MR, et al. MIRD pamphlet no. 22 (abridged): Radiobiology and dosimetry of α-particle emitters for targeted radionuclide therapy. J Nucl Med 2010;51:311.
7. Graf F, Fahrer J, Maus S, et al. DNA double strand breaks as predictor of efficacy of the alpha-particle emitter Ac-225 and the electron emitter Lu-177 for somatostatin receptor targeted radiotherapy. PLoS One 2014;9:e88239.
8. Nikula TK, McDevitt MR, Finn RD, et al. Alpha-emitting bismuth cyclohexylbenzyl DTPA constructs of recombinant humanized anti-CD33 antibodies: Pharmacokinetics, bioactivity, toxicity and chemistry. J Nucl Med 1999;40:166.
9. Kluetz PG, Pierce W, Maher VE, et al. Radium Ra 223 dichloride injection: U.S. food and drug administration drug approval summary. Clin Cancer Res 2014;20:9.
10. Shirley M, McCormack PL. Radium-223 dichloride: A review of its use in patients with castration-resistant prostate cancer with symptomatic bone metastases. Drugs 2014;74:579.
11. Coleman R. Treatment of metastatic bone disease and the emerging role of radium-223. Semin Nucl Med 2016; 46:99.
12. Kim Y-S, Brechbiel MW. An overview of targeted alpha therapy. Tumor Biol 2012;33:573.
13. Dekempeneer Y, Keyaerts M, Krasniqi A, et al. Targeted alpha therapy using short-lived alpha-particles and the promise of nanobodies as targeting vehicle. Expert Opin Biol Ther 2016;16:1035.
14. Makvandi M, Dupis E, Engle JW, et al. Alpha-emitters and targeted alpha therapy in oncology: From basic science to clinical investigations. Target Oncol 2018;13: 189.
15. Price EW, Orvig C. Matching chelators to radiometals for radiopharmaceuticals. Chem Soc Rev 2014;43:260.
16. Geerlings MW, Kaspersen FM, Apostolidis C, et al. The feasibility of ^{225}Ac as a source of alpha-particles in radioimmunotherapy. Nucl Med Commun 1993;14:121.
17. Miederer M, Scheinberg DA, McDevitt MR. Realizing the potential of the Actinium-225 radionuclide generator in targeted alpha particle therapy applications. Adv Drug Deliv Rev 2008;60:1371.

18. Scheinberg DA, McDevitt MR. Actinium-225 in targeted alpha-particle therapeutic applications. Curr Radiopharm 2011;4:306.
19. Pommé S, Marouli M, Suliman G, et al. Measurement of the ^{225}Ac half-life. Appl Radiat Isot 2012;70:2608.
20. Chart of Nuclides. Maintained by the National Nuclear Data Center at Brookhaven National Lab. Online document at www.nndc.bnl.gov/chart Accessed on May 6, 2018.
21. McDevitt MR, Barendswaard E, Ma D, et al. An α-particle emitting antibody ([^{213}Bi]J591) for radioimmunotherapy of prostate cancer. Cancer Res 2000;60:6095.
22. McDevitt MR, Ma D, Lai LT, et al. Tumor therapy with targeted atomic nanogenerators. Science 2001;294:1537.
23. Song H, Hobbs RF, Vajravelu R, et al. Radioimmunotherapy of breast cancer metastases with α-particle emitter ^{225}Ac: Comparing efficacy with ^{213}Bi and ^{90}Y. Cancer Res 2009; 69:8941.
24. Boll RA, Malkemus D, Mirzadeh S. Production of actinium-225 for alpha particle mediated radioimmunotherapy. Appl Radiat Isot 2005;62:667.
25. Apostolidis C, Molinet R, Rasmussen G, et al. Production of Ac-225 from Th-229 for targeted α therapy. Anal Chem 2005;77:6288.
26. Apostolidis C, Molinet R, McGinley J, et al. Cyclotron production of Ac-225 for targeted alpha therapy. Appl Radiat Isot 2005;62:383.
27. Zhuikov BL, Kalmykov SN, Ermolaev SV, et al. Production of ^{225}Ac and ^{223}Ra by irradiation of Th with accelerated protons. Radiochemistry 2011;53:73.
28. Weidner JW, Mashnik SG, John KD, et al. ^{225}Ac and ^{223}Ra production via 800 MeV proton irradiation of natural thorium targets. Appl Radiat Isot 2012;70:2590.
29. Engle JW, Mashnik SG, Weidner JW, et al. Cross sections from proton irradiation of thorium at 800 MeV. Phys Rev C Nucl Phys 2013;88:014604.
30. Hoehr C, Bénard F, Buckley K, et al. Medical isotope production at TRIUMF—From imaging to treatment. Phys Procedia 2017;90:200.
31. Henriksen G, Schoultz BW, Michaelsen TE, et al. Sterically stabilized liposomes as a carrier for α-emitting radium and actinium radionuclides. Nucl Med Biol 2004; 31:441.
32. Fitzsimmons J, Atcher R. Synthesis and evaluation of a water-soluble polymer to reduce Ac-225 daughter migration. J Labelled Comp Radiopharm 2007;50:147.
33. Woodward J, Kennel SJ, Stuckey A, et al. $LaPO_4$ nanoparticles doped with actinium-225 that partially sequester daughter radionuclides. Bioconjugate Chem 2011;22:766.
34. McLaughlin MF, Woodward J, Boll RA, et al. Gold coated lanthanide phosphate nanoparticles for targeted alpha generator radiotherapy. PLoS One 2013;8:e54531.
35. Bandekar A, Zhu C, Jindal R, et al. Anti-prostate-specific membrane antigen liposomes loaded with ^{225}Ac for potential targeted antivascular α-particle therapy of cancer. J Nucl Med 2014;55:107.
36. Matson ML, Villa CH, Ananta JS, et al. Encapsulation of α-particle-emitting $^{225}Ac^{3+}$ ions within carbon nanotubes. J Nucl Med 2015;56:897.
37. de Kruijff RM, Drost K, Thijssen L, et al. Improved ^{225}Ac daughter retention in $InPO_4$ containing polymersomes. Appl Radiat Isot 2017;128:183.
38. Cękedrowska E, Pruszynski M, Majkowska-Pilip A, et al. Functionalized TiO_2 nanoparticles labelled with ^{225}Ac for targeted alpha radionuclide therapy. J Nanopart Res 2018; 20:83.
39. Kirby HW. The discovery of actinium. Isis 1971;62:290.
40. Fry C, Thoennessen M. Discovery of actinium, thorium, protactinium, and uranium isotopes. At Data Nucl Data Tables 2013;99:345.
41. ENSDF, Evaluated Nuclear Structure Data File. Maintained by the National Nuclear Data Center at Brookhaven National Lab. Online document at www.nndc.bnl.gov/ensdf Accessed on March 17, 2018.
42. Kirby HW, Morss LR. Actinium. In: Morss LR, Edelstein NM, Fuger J (eds.), The Chemistry of the Actinide and Transactinide Elements. Dordrecht: Springer Netherlands, 2006;18.
43. Yamana H, Mitsugashira T, Shiokawa Y, et al. Possibility of the existence of divalent actinium in aqueous solution. J Radioanal Chem 1983;76:19.
44. Malý J. The amalgamation behavior of heavy elements—III Extraction of radium, lead and the actinides by sodium amalgam from acetate solutions. J Inorg Nucl Chem 1969; 31:1007.
45. Nugent LJ, Baybarz RD, Burnett JL, et al. Electron-transfer and f-d absorption bands of some lanthanide and actinide complexes and the standard (II-III) oxidation potential for each member of the lanthanide and actinide series. J Phys Chem 1973;77:1528.
46. Bratsch SG, Lagowski JJ. Actinide thermodynamic predictions. 3. Thermodynamics of compounds and aquo ions of the 2+, 3+, and 4+ oxidation states and standard electrode potentials at 298.15 K. J Phys Chem 1986;90:307.
47. Shannon RD. Revised effective ionic radii and systematic studies of interatomic distances in halides and chalcogenides. Acta Cryst A 1976;32:751.
48. Ziv DM, Shestakova IA. Investigation of the solubility of certain actinium compounds. II. Determination of the solubility and evaluation of the relative basicity of actinium hydroxide. Sov Radiochem 1965;7:176.
49. Baes CF, Mesmer RE. The Hydrolysis of Cations. New York: Wiley, 1976.
50. Kulikov E, Novgorodov A, Schumann D. Hydrolysis of ^{225}Actinium trace quantities. J Radioanal Nucl Chem 1992;164:103.
51. Zielińska B, Bilewicz A. The hydrolysis of actinium. J Radioanal Nucl Chem 2004;261:195.
52. Pearson RG. Hard and soft acids and bases. J Am Chem Soc 1963;85:3533.
53. Parr RG, Pearson RG. Absolute hardness: Companion parameter to absolute electronegativity. J Am Chem Soc 1983;105:7512.
54. Pearson RG. Absolute electronegativity and hardness: Application to inorganic chemistry. Inorg Chem 1988; 27:734.
55. Cotton S. Introduction to the actinides. In: Cotton S (ed.), Lanthanide and Actinide Chemistry. Chichester: John Wiley & Sons, Ltd, 2006;145.
56. Drago RS, Vogel GC, Needham TE. A four-parameter equation for predicting enthalpies of adduct formation. J Am Chem Soc 1971;93:6014.
57. Hancock RD, Marsicano F. Parametric correlation of formation constants in aqueous solution. 1. Ligands with small donor atoms. Inorg Chem 1978;17:560.
58. Hancock RD, Marsicano F. Parametric correlation of formation constants in aqueous solution. 2. Ligands with large donor atoms. Inorg Chem 1980;19:2709.

59. Aziz A, Lyle SJ. Complexes of lanthanum and actinium with fluoride, oxalate and sulphate in aqueous solutions. J Inorg Nucl Chem 1970;32:1925.
60. Shahani CJ, Mathew KA, Rao CL, et al. Chemistry of actinium. I. Stability constants of chloride, bromide, nitrate and sulphate complexes. Radiochim Acta 1968;10:165.
61. Rao CL, Shahani CJ, Mathew KA. Chemistry of actinium—II Stability constants of thiocyanate complexes of actinium and lanthanum. Inorg Nucl Chem Lett 1968;4:655.
62. Sekine T, Sakairi M. Studies of actinium(III) in various solutions. III. Actinium (III) complexes with oxalate, sulfate, chloride, and thiocyanate ions in perchlorate media. Bull Chem Soc Jpn 1969;42:2712.
63. Rao VK, Shahani CJ, Rao CL. Studies on the phosphate complexes of actinium and lanthanum. Radiochim Acta 1970;14:31.
64. Alleluia IB, Eberle SH, Keller C, Kirby HW. Gmelin Handbook of Inorganic Chemistry, Actinium, 8th ed., In: Kugler HK, Keller C (eds.), system no. 40 suppl. vol. 1. Berlin: Springer-Verlag, 1981.
65. Makarova TP, Sinitsyna GS, Stepanov AV, et al. Complex formation of actinium. I. Determination of the stability constants of ethylenediaminetetraacetate complexes of actinium and its separation from lanthanum in solutions of EDTA by the method of electromigration. Sov Radiochem 1972;14:555.
66. Smith RM, Martell AE. Iminodiacetic Acid Derivatives. In: Martell AE, Smith RM (eds.), Critical Stability Constants: Second Supplement. Boston: Springer, 1989;67.
67. Smith RM, Martell AE. Carboxylic acids. In: Martell AE, Smith RM (eds.), Critical Stability Constants: Second Supplement. Boston: Springer, 1989;299.
68. Fried S, Hagemann F, Zachariasen WH. The preparation and identification of some pure actinium compounds. J Am Chem Soc 1950;72:771.
69. Weigel F, Hauske H. The lattice constants of actinium(III) oxalate deca-hydrate. J Less Common Met 1977;55:243.
70. Farr JD, Giorgi AL, Bowman MG, et al. The crystal structure of actinium metal and actinium hydride. J Inorg Nucl Chem 1961;18:42.
71. Ferrier MG, Batista ER, Berg JM, et al. Spectroscopic and computational investigation of actinium coordination chemistry. Nat Commun 2016;7:12312.
72. Ferrier MG, Stein BW, Batista ER, et al. Synthesis and characterization of the actinium aquo ion. ACS Cent Sci 2017;3:176.
73. Allen PG, Bucher JJ, Shuh DK, et al. Coordination chemistry of trivalent lanthanide and actinide ions in dilute and concentrated chloride solutions. Inorg Chem 2000;39:595.
74. Durbin PW. Metabolic characteristics within a chemical family. Health Phys 1959;2:225.
75. Davis IA, Glowienka KA, Boll RA, et al. Comparison of ^{225}actinium chelates: Tissue distribution and radiotoxicity. Nucl Med Biol 1999;26:581.
76. Deal KA, Davis IA, Mirzadeh S, et al. Improved in vivo stability of actinium-225 macrocyclic complexes. J Med Chem 1999;42:2988.
77. McDevitt MR, Ma D, Simon J, et al. Design and synthesis of ^{225}Ac radioimmunopharmaceuticals. Appl Radiat Isot 2002;57:841.
78. Borchardt PE, Yuan RR, Miederer M, et al. Targeted actinium-225 in vivo generators for therapy of ovarian cancer. Cancer Res 2003;63:5084.
79. Miederer M, McDevitt MR, Sgouros G, et al. Pharmacokinetics, dosimetry, and toxicity of the targetable atomic generator, ^{225}Ac-HuM195, in nonhuman primates. J Nucl Med 2004;45:129.
80. Jaggi JS, Henke E, Seshan SV, et al. Selective alpha-particle mediated depletion of tumor vasculature with vascular normalization. PLoS One 2007;2:e267.
81. Miederer M, Henriksen G, Alke A, et al. Preclinical evaluation of the α-particle generator nuclide ^{225}Ac for somatostatin receptor radiotherapy of neuroendocrine tumors. Clin Cancer Res 2008;14:3555.
82. Escorcia FE, Henke E, McDevitt MR, et al. Selective killing of tumor neovasculature paradoxically improves chemotherapy delivery to tumors. Cancer Res 2010;70:9277.
83. Essler M, Gärtner FC, Neff F, et al. Therapeutic efficacy and toxicity of ^{225}Ac-labelled vs. ^{213}Bi-labelled tumour-homing peptides in a preclinical mouse model of peritoneal carcinomatosis. Eur J Nucl Med Mol Imaging 2012;39:602.
84. Maguire WF, McDevitt MR, Smith-Jones PM, et al. Efficient 1-step radiolabeling of monoclonal antibodies to high specific activity with ^{225}Ac for α-particle radioimmunotherapy of cancer. J Nucl Med 2014;55:1492.
85. Majkowska-Pilip A, Rius M, Bruchertseifer F, et al. In vitro evaluation of ^{225}Ac-DOTA-substance P for targeted alpha therapy of glioblastoma multiforme. Chem Biol Drug Des 2018. DOI:10.1111/cbdd.13199.
86. Pruszynski M, D'Huyvetter M, Bruchertseifer F, et al. Evaluation of an anti-HER2 nanobody labeled with ^{225}Ac for targeted α-particle therapy of cancer. Mol Pharmaceutics 2018;15:1457.
87. Jurcic JG, Rosenblat TL, McDevitt MR, et al. Targeted alpha-particle nano-generator actinium-225 (^{225}Ac)-lintuzumab (anti-CD33) in acute myeloid leukemia (AML). Clin Lymphoma Myeloma Leuk 2013;13:S379.
88. Jurcic JG, Ravandi F, Pagel JM, et al. Phase I trial of α-particle therapy with actinium-225 (^{225}Ac)-lintuzumab (anti-CD33) and low-dose cytarabine (LDAC) in older patients with untreated acute myeloid leukemia (AML). J Clin Oncol 2015;33:7050.
89. Kratochwil C, Bruchertseifer F, Giesel FL, et al. ^{225}Ac-PSMA-617 for PSMA-targeted α-radiation therapy of metastatic castration-resistant prostate cancer. J Nucl Med 2016;57:1941.
90. Kratochwil C, Bruchertseifer F, Rathke H, et al. Targeted α-therapy of mCRPC with ^{225}Ac-PSMA-617: Dosimetry estimate and empirical dose finding. J Nucl Med 2017;58:1624.
91. Smith RM, Martell AE. Aminocarboxylic acids. In: Martell AE, Smith RM (eds.), Critical Stability Constants: Second Supplement. Boston: Springer, 1989;1.
92. Wu SL, Horrocks WD. Direct determination of stability constants of lanthanide ion chelates by laser-excited europium(III) luminescence spectroscopy: Application to cyclic and acyclic aminocarboxylate complexes. J Chem Soc Dalton Trans 1997:1497.
93. Kelly JM, Amor-Coarasa A, Nikolopoulou A, et al. Assessment of PSMA targeting ligands bearing novel chelates with application to theranostics: Stability and complexation kinetics of $^{68}Ga^{3+}$, $^{111}In^{3+}$, $^{177}Lu^{3+}$ and $^{225}Ac^{3+}$. Nucl Med Biol 2017;55:38.
94. Beyer GJ, Bergmann R, Schomäcker K, et al. Comparison of the biodistribution of ^{225}Ac and radio-lanthanides

as citrate complexes. Isotopes Environ Health Stud 1990; 26:111.
95. Beyer GJ, Offord RE, Künzi G, et al. Biokinetics of monoclonal antibodies labelled with radio-lanthanides and 225-Ac in xenografted nude mice: Preliminary results. J Labelled Comp Radiopharm 1995;37:529.
96. Beyer GJ, Offord R, Künzi G, et al. The influence of EDTMP-concentration on the biodistribution of radiolanthanides and 225-Ac in tumor-bearing mice. Nucl Med Biol 1997;24:367.
97. Chappell LL, Deal KA, Dadachova E, et al. Synthesis, conjugation, and radiolabeling of a novel bifunctional chelating agent for ^{225}Ac radioimmunotherapy applications. Bioconjugate Chem 2000;11:510.
98. Kennel SJ, Chappell LL, Dadachova K, et al. Evaluation of ^{225}Ac for vascular targeted radioimmunotherapy of lung tumors. Cancer Biother Radiopharm 2000;15:235.
99. Hancock RD. Chelate ring size and metal ion selection. The basis of selectivity for metal ions in open-chain ligands and macrocycles. J Chem Educ 1992;69:615.
100. Chen X, Ji M, Fisher DR, et al. Carboxylate-derived calixarenes with high selectivity for actinium-225. Chem Commun 1998:377.
101. Chen X, Ji M, Fisher DR, et al. Monofunctionalization of calix[4]arene tetracarboxylic acid at the upper rim with isothiocyanate group: First bifunctional chelating agent for alpha-emitter Ac-225. Synlett 1999;11:1784.
102. Grote Gansey MHB, de Haan AS, Bos ES, et al. Conjugation, immunoreactivity, and immunogenicity of calix[4]arenes; model study to potential calix[4]arene-based Ac^{3+} chelators. Bioconjugate Chem 1999;10:613.
103. Preihs C, Arambula JF, Magda D, et al. Recent developments in texaphyrin chemistry and drug discovery. Inorg Chem 2013;52:12184.
104. Cao X, Li Q, Moritz A, et al. Density functional theory studies of actinide(III) motexafins (An-Motex^{2+}, An = Ac, Cm, Lr). Structure, stability, and comparison with lanthanide(III) motexafins. Inorg Chem 2006;45:3444.
105. Thiabaud G, Radchenko V, Wilson JJ, et al. Rapid insertion of bismuth radioactive isotopes into texaphyrin in aqueous media. J Porphyrins Phthalocyanines 2017;21:882.
106. Preihs C, Arambula JF, Lynch VM, et al. Bismuth- and lead-texaphyrin complexes: Towards potential α-core emitters for radiotherapy. Chem Commun 2010;46:7900.
107. Wilson JJ, Ferrier M, Radchenko V, et al. Evaluation of nitrogen-rich macrocyclic ligands for the chelation of therapeutic bismuth radioisotopes. Nucl Med Biol 2015;42:428.
108. Comba P, Jermilova U, Orvig C, et al. Octadentate picolinic acid-based bispidine ligand for radiometal ions. Chem Eur J 2017;23:15945.
109. Thiele NA, Brown V, Kelly JM, et al. An eighteen-membered macrocyclic ligand for actinium-225 targeted alpha therapy. Angew Chem Int Ed 2017;56:14712.
110. Roca-Sabio A, Mato-Iglesias M, Esteban-Gómez D, et al. Macrocyclic receptor exhibiting unprecedented selectivity for light lanthanides. J Am Chem Soc 2009;131:3331.
111. Boubekeur-Lecaque L, Souffrin C, Gontard G, et al. Water soluble diaza crown ether derivative: Synthesis and barium complexation studies. Polyhedron 2014;68:191.
112. Chong H-S. Multifunctional chelators, complexes, and compositions thereof, and methods of using same. PCT Int Appl WO 2015051362 A1, 2015.